Environmental Pollution xxx (2018) xxx-xxx

Contents lists available at ScienceDirect

Environmental Pollution

journal homepage: www.elsevier.com

Long-term field evaluation of the plantower PMS low-cost particulate matter sensors☆

T. Sayahi*, A. Butterfield, K.E. Kelly

University of Utah, Department of Chemical Engineering, 3290 MEB, 50 S. Central Campus Dr, Salt Lake City, UT, United States

ARTICLE INFO

Article history:
Received 13 April 2018
Received in revised form 13 November 2018
Accepted 21 November 2018
Available online xxx

Keywords:
Particulate matter
Air quality
Low-cost sensors
Cold-air pools
Wildfires

ABSTRACT

The low-cost and compact size of light-scattering-based particulate matter (PM) sensors provide an opportunity for improved spatiotemporally resolved PM measurements. However, these inexpensive sensors have limitations and need to be characterized under realistic conditions. This study evaluated two Plantower PMS (particulate matter sensor) 1003s and two PMS 5003s outdoors in Salt Lake City, Utah over 320 days (1/2016–2/2016 and 12/2016–10/2017) through multiple seasons and a variety of elevated $PM_{2.5}$ events including wintertime cold-air pools (CAPs), fireworks, and wildfires. The PMS 1003/5003 sensors generally tracked $PM_{2.5}$ concentrations compared to co-located reference air monitors (one tapered element oscillating microbalance, TEOM, and one gravimetric federal reference method, FRM). The different PMS sensor models and sets of the same sensor model exhibited some intra-sensor variability. During winter 2017, the two PMS 1003s consistently overestimated $PM_{2.5}$ by a factor of 1.89 (TEOM $PM_{2.5}$<40 μg/m^3). However, compared to the TEOM, one PMS 5003 overestimated $PM_{2.5}$ concentrations by a factor of 1.47 while the other roughly agreed with the TEOM. The PMS sensor response also differed by season. In two consecutive winters, the PMS $PM_{2.5}$ measurements correlated with the hourly TEOM measurements (R^2>0.87) and 24-h FRM measurements (R^2>0.88) while in spring (March–June) and wildfire season (June–October) 2017, the correlations were poorer (R^2 of 0.18–0.32 and 0.48–0.72, respectively). The PMS 1003s maintained high intra-sensor agreement after one year of deployment during the winter seasons, however, one PMS 1003 sensor exhibited a significant drift beginning in March 2017 and continued to deteriorate through the end of the study. Overall, this study demonstrated good correlations between the PMS sensors and reference monitors in the winter season, seasonal differences in sensor performance, some intra-sensor variability, and drift in one sensor. These types of factors should be considered when using measurements from a network of low-cost PM sensors.

1. Introduction

Fine particulate matter (PM), with an aerodynamic diameter less than 2.5 μm ($PM_{2.5}$), is a concern due to its adverse environmental and health effects, including heart attacks, decreased lung and cognitive function and premature death (Brook et al., 2010; Raaschou-Nielsen et al., 2013; Weuve et al., 2012). The combination of emission sources and atmospheric conditions can create levels of $PM_{2.5}$ that greatly exceed World Health Organization (WHO) or the United States Environmental Protection Agency (U.S. EPA) ambient air-quality standards, and this in turn causes significant health and economic burdens. For example, wildfires can cause the daily average of $PM_{2.5}$ levels of up to 100 μg/m^3, more than 2.75 times the 24-h U.S. EPA National Ambient Air Quality Standard (NAAQS) of 35 μg/m^3 (Hänninen et al., 2009; Holstius et al., 2012; Kolbe and Gilchrist, 2009; Kunii et al., 2002). Festival fireworks, such as Diwali in India, the Lantern Festival in China and the Independence Day in the U.S., are also associated with elevated $PM_{2.5}$ levels. For example, Barman et al. (2009) measured 24-h $PM_{2.5}$ levels of 352 μg/m^3 in Vikas Negar, India, during Diwali (November 1, 2005). Enhancing public awareness of PM_{10} and $PM_{2.5}$ levels during pollution events can persuade the citizens to consider the necessary measures to reduce their PM exposure and consequently health risks.

In an effort to protect the health of its citizens, governmental agencies have developed ambient air-quality standards and have organized monitoring networks to track air quality (Vahlsing and Smith, 2012). Conventionally, government organizations and researchers monitor ambient PM concentrations at sparsely distributed stations with advanced instrumentation and/or filter-based protocols, including EPA federal reference methods (FRM) and federal-equivalent methods (FEM). Even though these methods meet regulatory requirements and assure measurement precision, accuracy, and consistency, the high cost and maintenance requirements of FRM/FEMs make it difficult to deploy many monitors. Consequently, they may not accurately capture the localized $PM_{2.5}$ gradients within a city or provide sufficient resolution for epidemiological studies (Health Effects Institute, 2010; Steinle et al., 2013). Therefore, alternative methods

☆ This paper has been recommended for acceptance by Charles Wong.

* Corresponding author..
Email address: tofighsayahi@chemeng.utah.edu (T. Sayahi)

https://doi.org/10.1016/j.envpol.2018.11.065
0269-7491/

are needed to complement traditional spatially dispersed air-quality networks. The recent availability of low-cost, light-scattering PM sensors could improve PM measurement density and help individuals reduce their individual PM exposure. These sensors are low-power, compact, portable and inexpensive (<$500). Several organizations have begun measuring and reporting PM measurements from low-cost sensor networks, including PurpleAir and CAIRSENSE (Jiao et al., 2016; PurpleAir, 2018). However, presenting readings from these types of sensors, without corresponding calibration and data-quality metrics, may result in either unjustified public contentment or concern (Shapiro et al., 2014).

These inexpensive sensors have limitations, and not all of them provide meaningful air quality data (Williams et al., 2014). Their precision and accuracy are not as good as FEMs (Shapiro et al., 2014). Detection sensitivity may be a limitation, and one study reports that PM measurements can be influenced by humidity (Wang et al., 2015). Standards do not yet exist for evaluating the performance of these low-cost PM sensors, and limited performance information is provided by the vendors. Researchers have begun to fill in this gap by assessing the performance of various PM sensors under different environmental and controlled conditions (Dinoi et al., 2017; Gao et al., 2015; Papapostolou et al., 2017; Patel et al., 2017; Wang et al., 2015). Manikonda et al. (2016) conducted a laboratory experiment in a room-sized laboratory chamber with standard conditions of temperature and relative humidity (RH) using two sources of PM (Arizona Test Dust and cigarette smoke) to assess the performance of four inexpensive PM sensors (TSI AirAssure, Dylos, UB AirSense, and Speck) in comparison to three research-grade instruments (a TSI FMPS 3091, a TSI APS 3321, and a Grimm 1.109). The results indicated that only one of the three AirAssure sensors correlated well ($R^2 = 0.990$) with APS 3321 PM measurements; this illustrates that even sets of the same low-cost sensor can lack precision. Gao et al. (2015) and Wang et al. (2014) also report that low-cost sensors can lack precision. Although laboratory evaluations of low-cost sensors can provide promising results, they typically fail to reflect the variability of pollution and meteorological conditions existing in the real-world (Jovašević-Stojanović et al., 2015; Li and Biswas, 2017; Liu et al., 2017; Mukherjee et al., 2017; Piedrahita et al., 2014; Sousan et al., 2017, 2016).

Few field studies have examined sensor performance over extended periods of time. One notable exception is an 8-month assessment of five types of low-cost, PM sensors (Shinyei, Dylos, Airbeam, MetOne, and Air Quality Egg) by Jiao et al. (2016) in a low-pollution suburban environment. They found high agreement between the low-cost sensors of the same type ($R^2 = 0.980$), however, moderate correlation with a $PM_{2.5}$ reference monitor ($R^2 = 0.420$). Several field studies have examined sensor performance over time periods of days to weeks. For example, in a 4-day field study, Gao et al. (2015) tested the performance of a Shinyei sensor in highly polluted urban areas of China (24-h $PM_{2.5}$ 330–413 μg/m^3). The results revealed good to moderate correlations to co-located reference platforms, a DustTrak II model 8532 ($R^2 = 0.860$–0.890) and a filter-based 24-h gravimetric $PM_{2.5}$ monitor, Airmetrics MiniVol Tactical Air Sampler, ($R^2 = 0.530$). In Oakland California, Holstius et al. (2014) compared the 24-h measurements of a battery-operated Shinyei sensor with a 24-h BAM-1020 in a long-term evaluation (107-day period, $R^2 = 0.740$, and $PM_{2.5}$ concentration range of 0–20 μg/m^3). In an urban residential area of Houston Texas, Han et al. (2017) compared the 1-min average $PM_{2.5}$ measurement of a Dylos DC 1700 PM instrument with a Grimm 11-R (as a reference monitor) for 12 days ($PM_{2.5}$ 0.1–50.0 μg/m^3) and found a linear correlation ($R^2 = 0.778$).

This study aims to assess the performance of two models of the low-cost Plantower particulate matter sensor (PMS) 1003 and 5003 in terms of accuracy, precision, limit of detection, and variation/noise over a long-time period (320 days) under a variety of ambient conditions, including several high PM episodes in Salt Lake City, Utah caused by CAPs, wildfires and fireworks. During these episodes, daily $PM_{2.5}$ levels can reach double the 24-h average NAAQS of 35 μg/m^3 and have adverse health consequences for the residents of the region, including increased risk of asthma (Beard et al., 2012), heart attack (Pope et al. (2006) and pre-term birth (Hackmann and Sjöberg, 2017).

2. Materials and methods

This investigation assessed the performance of the Plantower PMS 1003 over 320 days (January 6 to February 17, 2016 and December 16, 2016 to October 31 2017) during periodic episodes of high PM levels, such as several CAPs, fireworks and wildfires. During the course of this study, Plantower released a new sensor model, the PMS 5003 ($20), and during the second year, data were also collected with this new sensor. The PMS 5003 operates on the same principal as the PMS 1003, described in Kelly et al. (2017). The PMS 5003 measures 90-degree light scattering with a photo-diode detector that converts scattered light to a voltage pulse. The PMS 5003's light source is a laser that operates at a wavelength of 680 ± 10 nm (measured by a Lambda 35 spectrophotometer, PerkinElmer, Inc). The particle number is calculated by counting the pulses from the scattering signal. The manufacturer uses a proprietary algorithm to convert the number of pulses to PM concentration. A fan draws air past the laser at a flow rate of approximately 0.1 L/min. According to the manufacturer, both PMS sensors have a response time of less than 10 seconds, which suggests that the sensors have limitations in quick changing environments. They report the sensor's mean time to failure is more than three years, and its detection range is 0–500 μg/m^3. For the concentration ranges of 0–100 μg/m^3 and 100–500 μg/m^3 uncertainties are ±10 μg/m^3 and ±10%, respectively. Moreover, the working temperature and RH ranges of the sensors are −10∼+60 °C and 0–99%, respectively. The PMS 1003/5003 sensor provides PM_1, $PM_{2.5}$ and PM_{10} mass concentration with two correction factors, CF = 1 (for laboratory evaluations) and CF = atmos (for field evaluations). Details of the CF atmos factor are not available from the manufacturer; consequently, we performed our analysis on results using CF = 1. The PMS 5003 differs slightly from the PMS 1003 model in the flow pattern (position of the entrance and the laser alignment, Fig. 1) and the laser wavelength (650 ± 10 nm for PMS 1003).

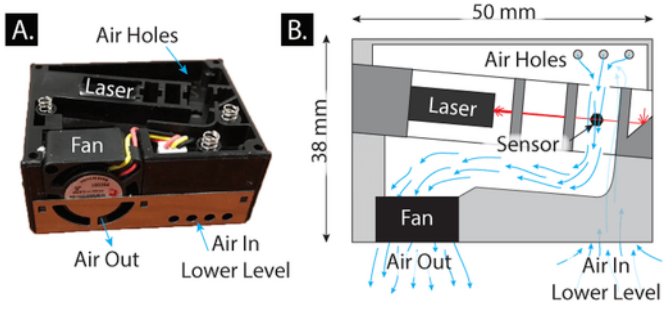

Fig. 1. (A) Plantower PMS 5003 (B) schematic of Plantower PMS 5003 sensor. The sensor is split into two layers. Air enters on the lower level, travels under the laser stage and emerges through holes on the laser's level. The air then travels into the laser's path, and scattered light is used to estimate PM concentration. A small DC fan draws air through the device.

PurpleAir, a local community organization, operates a sensor network based on the PMS sensors. They provided two new PurpleAir I (PMS 1003) and one new PurpleAir II (PMS 5003) for the evaluation. The PurpleAirII contains two PMS 5003 sensors mounted in one housing. Both PurpleAir sensor models contain: a BME280 pressure, temperature and humidity sensor, and an ESP8266 chip to communicate with the PMS sensor and to communicate over WiFi to their cloud database. The firmware receives PM_1, $PM_{2.5}$ and PM_{10} concentrations every second and averages the readings every 20 seconds. (PurpleAir, 2018).

2.1. Limit of detection (LOD)

The Kaiser and Specker (1956) method was utilized to estimate the LODs for PMS 1003/5003:

$$LOD = \frac{3\sigma_{blk}}{k} \quad (1)$$

where σ_{blk} is the standard deviation of the sensor's output at blank conditions. In this study, blank measurements occur when the hourly co-located reference $PM_{2.5}$ concentration (FEM) was less than 1 μg/m^3. This corresponds to 87, 152, and 105 for $PM_{2.5}$ and 46, 68, and 19 for PM_{10} measurements for winter, spring, and wildfire seasons, respectively. k is the slope of the linear relationship for each PMS sensor versus FEM concentrations (fit 3, Tables S–1).

2.2. Sensor bias

The bias of the PMS sensors was determined as a ratio between each of the PMS sensor readings at time t (PMS_t) and the reference concentration at time t (Ref_t) for each of the hourly measurement points:

$$Bias_t = \left(\frac{PMS_t}{Ref_t} - 1\right) \times 100 \quad (2)$$

The normalized root mean square error (*NormRMSE*) was calculated for each sensor:

$$NormRMSE = 100 \times \frac{RMSE}{\overline{Ref}} \quad (3)$$

$$RMSE = \sqrt{\frac{1}{N}\sum_{1}^{N}\left(PMS_t - Ref_t\right)^2} \quad (4)$$

where *NormRMSE* is the normalized root mean square error, *RMSE* is the root mean square error of sensor readings at each time (PMS_t) over each season, $\overline{Ref}$ is the average of all the hourly reference values for each season, and N is the number of observations at each season.

2.3. Sensor residuals

The normalized residuals for the sensors were determined to assess the stability of each PMS sensor over time:

$$Res_t = \frac{Ref_t - PMS_t}{Ref_t} \quad (5)$$

in which, Res_t is the normalized residual for the sensor at time t.

2.4. Field evaluation

In this study, four PMS sensors of two different models (1003 and 5003) were co-located alongside a gravimetric FRM (Thermo Partisol™ 2025i Sequential Air Sampler) and an FEM (Thermo Scientific 1405-F tapered element oscillating microbalance, TEOM) at the Hawthorne state monitoring station (AQS: 49-035-3006) beginning in Dec 2016. This monitoring site is located in an urban residential neighborhood that lies 5 km south east of down town Salt Lake City, Utah (longitude: 111.8721, latitude: 40.7343, elevation:1312 m, Fig. S-1). Potentially significant sources in the vicinity include one adjacent 6-lane road, one rail yard (7.5 km south west) and two interstates (I-80, 1.6 km to the south, and I-15 3 km west). In this study, one-minute PMS sensor readings were averaged on an hourly or a 24-h basis for comparison with the FEM and FRMs.

Table 1 shows how the meteorological conditions and PM concentrations varied by season and year. It is worth noting that the average $PM_{2.5}$ concentration in winter 2017 is lower than that in winter of 2016. Wind roses from the monitoring station for each season can be found in the supplementary material (Fig. S-2). During winter, the wind comes primarily from the southeast and west. During spring and summer, the wind comes primarily from the northwest and southeast.

The seasons in Table 1 are defined based on the differences in $PM_{2.5}$ levels and compositions. Winter is characterized by periodic CAPs and by $PM_{2.5}$ composed primarily of secondary inorganic aerosols including ammonium nitrate, ammonium sulfate and ammonium chloride (Tables S–2). Wildfire season is characterized by periodic wildfire and firework impacts. During this season $PM_{2.5}$ has larger contributions from crustal material and organic carbon. Spring is characterized by low PM levels. These seasonal differences in composition agree with previous studies (Kelly et al., 2013).

Table 1 also contains the number of observations for each season. The FRM instrument was not operating for 11% of the 2017 study period, and this 11% included significant CAP events. In the Kelly et al. (2017) paper, the 2016 winter hourly TEOM concentrations were adjusted to obtain the same 24-h average as the 24-h FRM $PM_{2.5}$ concentration. However, this study did not adjust the hourly FEM so that a more complete $PM_{2.5}$ data set could be evaluated. Consequently, the results in this paper for 2016 differ slightly from the previous publication.

3. Results and discussion

3.1. LOD

Tables S–3 shows the $PM_{2.5}$ and PM_{10} PMS sensor LODs (calculated using Eq. (1)), which were calculated separately for each sensor during three seasons (winter, spring and wildfire seasons, 2017). These different time periods have different number of observations for which a TEOM measurement was less than 1 μg/m^3. In 2017, the

Table 1
Ambient meteorological conditions and PM concentrations during the course of the study.

Season		Hourly temperature (°C)	Hourly RH (%)	Hourly wind speed (km/h)	Hourly TEOM $PM_{2.5}$ (μg/m^3)	Hourly TEOM PM_{10} (μg/m^3)	24-h FRM $PM_{2.5}$ (μg/m^3)	24-h FRM PM_{10} (μg/m^3)
Winter 2016 1/6–2/17	Avg.	0.0	69.2	4.2	16.3	17.2	20.0	31.6
	Range	-9–15.9	26.6–88.6	0.3–21.3	0–72.5	0–140	1.5–59.2	4.0–79.0
	N	742	716	976	738	752	43	23
Winter 2017 12/16/16–2/28/17	Avg.	2.2	62.4	3.9	14.4	18.6	13.5	24.6
	Range	−13.5–21.0	17.0–92.9	0.6–19.4	0–74.8	0–102	1.30–45.5	4.0–66.0
	N	1701	1674	1692	1664	1345	50	42
Spring 2017 3/1–5/31	Avg.	12.9	45.1	4.7	4.1	10.4	4.0	14.2
	Range	−1.7–31.2	8.4–88.6	0.5–21.2	0–20.0	0–166	1.1–9.3	3.00–47.0
	N	2092	2104	2135	2071	2061	90	89
Wildfire 2017 6/1–10/31	Avg.	22.4	37.2	4.0	10.5	15.4	7.3	22.0
	Range	0.1–39.9	2.6–89.7	0.4–16.4	0–102	0–460	1.6–35.5	4.0–76.0
	N	3403	3446	3001	3224	3526	139	132

RH: relative humidity, TEOM: tapered element oscillating microbalance, FRM: federal reference method, Avg: average, N: number of samples.

PMS $PM_{2.5}$ LODs ranged from 2.62 to 11.5 μg/m^3, which lies in the range of reported LOD values for different low-cost sensors, 1–26.9 μg/m^3 (Austin et al., 2015; Wang et al., 2015). The LODs for the PMS 1003 in winter 2017 (3.93–5.48 μg/m^3, 150 readings) are lower than the 2016 1003 LODs (13.7–14.3 μg/m^3, 18 readings). This difference in LODs is likely due to the greater number of observations in 2017. In 2017, the PMS 1003-1 had the highest LOD (11.5 μg/m^3, spring season) because of a baseline drift, discussed further in sections 3.4-3.7. The LOD for PMS 1003–1 also illustrates how the LOD of the same sensor can change with the passage of time. The range of PM_{10} PMS sensor LODs in winter 2017 was 11.5–15.9 μg/m^3, however, lower slopes and poorer correlation between hourly PM_{10} TEOM and hourly PM_{10} PMS readings during spring and wildfire seasons (R^2 = 0.010–0.168, slope = 0.033–0.286) result in higher PM_{10} LODs (16.4–228 μg/m^3). It should be noted that the LODs for winter are more reliable due to broader ranges of PM concentrations and higher coefficients of determination for the linear fits (fit 3, Tables S–1). In general, the LOD for the PMS 1003/5003 seem to be suitable for measuring $PM_{2.5}$ when concentrations exceed 6 μg/m^3 and PM_{10} when concentrations exceed 16 μg/m^3. These LOD estimates are used subsequently in Section 3.2.

3.2. Comparison of 24-h measurements

Table 2 shows the correlations between 24-h FRM PM concentrations and the TEOM and PMS sensors during winter 2016, and during winter, spring and wildfire season of 2017. In both winters, $PM_{2.5}$ readings from the TEOM correlated well with the FRM measurements (R^2 = 0.993–0.994). The 24-h averaged PMS $PM_{2.5}$ measurements also showed a strong correlation with the FRM, R^2 of 0.884–0.972 (winter 2016 and 2017). These observed correlations are in range of those 24-h correlations reported by Zheng et al. (2018) for five Plantower PMS 3003 sensors and an E-BAM-9800 (reference monitor) during winter 2017 (50 days) at Duke University (R^2 = 0.90–0.94). However, they are higher than those reported by Holstius et al. (2014) for a Shinyei sensor and 24-h BAM-1020 measurements, R^2 = 0.74 (107-day period). In 2017, the PMS 1003s exhibited slightly higher correlations with the FRM $PM_{2.5}$ measurements than in 2016, but this may be due to a larger number of observations (32–33 in 2016 vs. 48 in 2017) or the smaller number of days when 24-h $PM_{2.5}$ concentrations exceeded 40 μg/m^3 (7 in 2016 compared to 3 in 2017). At $PM_{2.5}$ concentrations greater than 40 μg/m^3 during a CAP, the PMS sensors begin to exhibit nonlinear behavior.

Table 2
Coefficient of determination (R^2) between 24-h FRM PM mass concentrations and 24-h averaged co-located sensor measurements in winter of 2016 (Kelly et al., 2017) and winter, spring and wildfire seasons of 2017 (Fig. S-3).

year	Season	FRM	TEOM	1003–1	1003–2	5003–1	5003–2
2016	Winter	$PM_{2.5}$	0.994	0.884	0.887	–	–
		obs	46	32	33	–	–
		PM_{10}	0.911	0.860	0.909	–	–
		obs	22	19	18	–	–
2017	Winter	$PM_{2.5}$	0.993	0.958	0.972	0.971	0.969
		obs	50	48	48	48	48
		PM_{10}	0.802	0.678	0.676	0.701	0.696
		obs	33	33	33	33	33
	Spring	$PM_{2.5}$	0.654	0.185	0.262	0.419	0.484
		obs	90	81	82	82	82
		PM_{10}	0.615	0.001	0.058	0.145	0.136
		obs	89	80	81	82	82
	Wildfire	$PM_{2.5}$	0.895	0.434	0.775	0.758	0.776
		obs	139	143	143	143	143
		PM_{10}	0.961	0.187	0.302	0.311	0.308
		obs	132	136	136	136	136

Generally, the TEOM-FRM PM correlations in spring and wildfire seasons (R^2 of 0.654–0.895 for $PM_{2.5}$ and 0.615–0.961 for PM_{10}) were also not as good as during the winter seasons (R^2 of 0.993–0.994 for $PM_{2.5}$ and 0.802–0.911 for PM_{10}). Zhu et al. (2012) reported a similar discrepancy between TEOM and FRM, which was attributed to the loss of semi-volatile mass by FRM during warmer weather. The range of PM concentrations is generally lower in spring and wildfire seasons than in winter (Table 1). During spring, 86.7% of 24-h $PM_{2.5}$ concentrations are less than the 6 μg/m^3 LOD, and 62.9% of PM_{10} concentrations are less than the 16 μg/m^3 LOD. During winter and wildfire seasons, 48.0% and 43.9% (for $PM_{2.5}$) and 57.4% and 29.9% (for PM_{10}) are less than 6 and 16 μg/m^3, respectively. Another reason for the poorer correlations during wildfire season may be attributed to a higher proportion of coarser particles. The mean FRM $PM_{2.5}/PM_{10}$ ratio in spring and wildfire seasons are 0.286 and 0.336, respectively, which are significantly less than that in winter, 0.516 (Student's t-test, p-value < 0.001). PMS sensors are likely not very efficient at measuring larger PM particles because the particles must make three (in PMS 1003s) or two (in PMS 5003s) 90-degree turns before passing the laser/photodetector. PMS PM_{10} concentrations do not correlate as well with FRM PM_{10} measurements compared to the $PM_{2.5}$ measurements (R^2 of 0.676–0.701 in winter, 0.001–0.123 in spring and 0.187–0.311 in wildfire season, 2017). The PMS PM_{10} readings during wildfire season also did not correlated well with the FRM PM_{10} mass concentrations (R^2 = 0.187–0.311). In addition, the PMS1003-1 exhibited significant drift beginning in March 2017, and this contributes to the poor correlation during the wildfire season. This is discussed in sections 3.4-3.7.

3.3. Comparison of hourly measurements

Fig. 2 shows the scatter plots of hourly averaged $PM_{2.5}$ measurements from the TEOM and the different PMS sensors during winter 2017 (December 16th, 2016-Febuary 28th 2017). During this season, all the PMS sensors overestimated $PM_{2.5}$ when $PM_{2.5}$ levels exceed approximately 10 μg/m^3. As in 2016, the PMS sensors also began to show non-linear behavior when the TEOM $PM_{2.5}$ concentrations increase above 40 μg/m^3. Austin et al. (2015) and Wang et al. (2015) conducted laboratory evaluations of low-cost PM sensors over a range of concentrations (0–600 μg/m^3 and 0–1000 μg/m^3, respectively), and they also observed these non-linear responses at concentrations greater than 50 μg/m^3 and 100 μg/m^3, respectively. They showed that non-linearity was more apparent for small diameter particles (less than 600 nm) and ammonium nitrate particles. During CAPs in this region, the particles tend to have small mean diameters (below 900 nm, Baasandorj et al., 2018) and are primarily comprised of ammonium nitrate, ammonium sulfate and ammonium chloride (Tables S–2). Consequently, the PMS's nonlinear response during winter CAPs is not unexpected. After one year of deployment, the PMS 1003s still had a high intra-sensor correlation (R^2 = 0.974 in 2017, R^2 = 0.995 in 2016, Kelly et al., 2017). The new model sensors, PMS 5003s, correlated highly with each other as well (R^2 = 0.970). This high PMS intra-sensor correlation was also reported in a SQAMD study (SQAMD, 2016). Fig. 2 also shows that in winter 2017 the two different models of PMS sensors (1003s and 5003s) have high correlations with each other (R^2 = 0.921–0.989).

In the winter of 2016 and 2017, neither the TEOM nor the PMS $PM_{2.5}$ measurements showed much correlation with four measured meteorological factors: temperature (R^2 = 0.101–0.131), RH (R^2 = 0.092–0.142), wind speed (R^2 = 0.116–0.138), and wind direc-

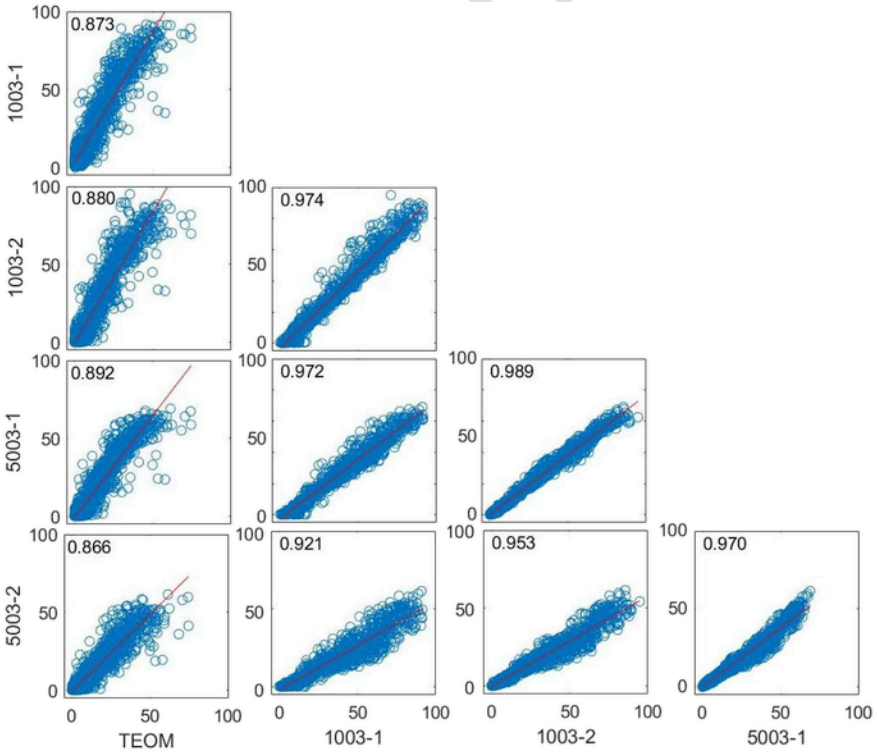

Fig. 2. Scatter plots and coefficients of determination for hourly $PM_{2.5}$ (μg/m^3) concentrations from the PMS 1003s and 5003s and an FEM (TEOM) in winter 2017.

tion (R^2 = 0.019–0.70). Holstius et al. (2014) also found negligible association between low-cost sensor measurements and temperature or RH in an ambient evaluation. However, in a laboratory evaluation, Wang et al. (2015) found no effect of temperature, but they found that that RH affects the responses of the three low-cost light scattering sensors they evaluated (Shinyei PPD42NS, Samyoung DSM501A, and Sharp GP2Y1010AU0F).

Fig. S-4 shows the hourly averaged TEOM and PMS PM_{10} concentrations for winter 2017. All the four sensors exhibit high intra-sensor correlations between the same and different models (R^2 = 0.925–0.987). In comparison to 2016, the PMS 1003 PM_{10} readings in 2017 did not correlate as well with the TEOM PM_{10} measurements (R^2 of 0.726–0.767 in 2017 vs. R^2 of 0.803–0.819 in 2016). One reason for the difference in 2016 and 2017 may be due to the total number of observations (752 in winter 2016 and 1345 in winter 2017, Table 1). As discussed in Section 3.2, the lower correlation between the PMS and the TEOM PM_{10} measurements may be due to the number of 90-degree turns that the particles must make before contacting the laser.

Fig. S-5-8 show the hourly averaged $PM_{2.5}$ and PM_{10} scatter plots for spring and wildfire seasons. The PMS shows poor correlations with TEOM readings in spring (R^2 of 0.183–0.324 for $PM_{2.5}$ and 0.010–0.123 for PM_{10}) and moderate/low correlations in wildfire season (R^2 of 0.538–0.724 for $PM_{2.5}$ and 0.114–0.168 for PM_{10}). As mentioned in section 3.2, for spring and wildfire season, a large proportion of the readings are at or below the sensor LODs and a larger fraction of coarse particles are present. In spite of the poor correlations with the TEOM, the 1003–2 and 5003s exhibit good intra-sensor correlations during spring (R^2 of 0.849–0.921 for $PM_{2.5}$ and 0.846–0.871 for PM_{10}) and wildfire season (R^2 of 0.915–0.979 for $PM_{2.5}$ and 0.940–0.978 for PM_{10}). However, the drifted sensor (1003–1) exhibits moderate correlations with the other three sensors (R^2 of 0.643–0.694 and 0.662–0.746 for $PM_{2.5}$ and 0.658–0.725 and 0.740–0.814 for PM_{10} in spring and wildfire seasons, respectively). In general, this study's results suggest that PMS sensors are not very good measures of PM_{10}.

3.4. Behavior during different PM events

From June through November, this region experiences periodic episodes of poor air quality due to fireworks, wildfires and dust storms. Fig. 3 and Figs. S-10-12 illustrate how the TEOM and PMS measurements track $PM_{2.5}$ and PM_{10} concentrations during these events. The fireworks on the 4th of July (Independence Day) and 24th of July (Pioneer Day) created spikes in the $PM_{2.5}$ concentration, which reached an hourly maximum of 29.0 μg/m^3 (TEOM). Several wildfires affected air quality, and this effect was confirmed by (a) the Utah Division of Air Quality requesting an exceptional event (Utah Division of Air Quality, 2017), (b) an increase in the contributions of organic carbon (Fig. S-9) to $PM_{2.5}$ concentrations, (c) wildfire activity reported by the Utah Department of Natural Resources, Utah Division of Forestry, Fire & State Lands, Salt Lake City, and (d) media referring to wildfires causing poor air quality during the period.

PM_{10} concentrations during the wildfire season show a pattern similar to $PM_{2.5}$ concentrations (Fig. S-10). One additional event provides further evidence of the PMS's poor response to PM_{10}. On October 20, 2017 the region experienced a dust storm (Lucie, 2017; Steenburgh, 2017), and TEOM PM_{10} reached 472 μg/m^3 while the co-located PMS sensors did not respond significantly to this event (Fig. S-11B).

Beginning in March, the PMS 1003–1 readings started to drift, and the $PM_{2.5}$ concentrations reported by this sensor were consistently higher than the $PM_{2.5}$ concentrations of the other sensors. Even during low-PM days, the PMS 1003–1 provided baseline measurements of 15 μg/m^3 rather than the 0–10 μg/m^3 range reported by the other sensors. The drift continued to get worse through the end of October.

3.5. Model fits

Various models were developed to describe the relationship between hourly TEOM and hourly averaged PMS $PM_{2.5}$ measurements. A linear, a fractional, an exponential, and a linear below 40 μg/m^3 models were evaluated by considering the goodness of fit metrics including R^2, RMSE (Tables S–1) and how the fits represent the actual data in regions with sparse data. The results show that the linear below 40 μg/m^3 and the exponential fits are the best fits to describe the

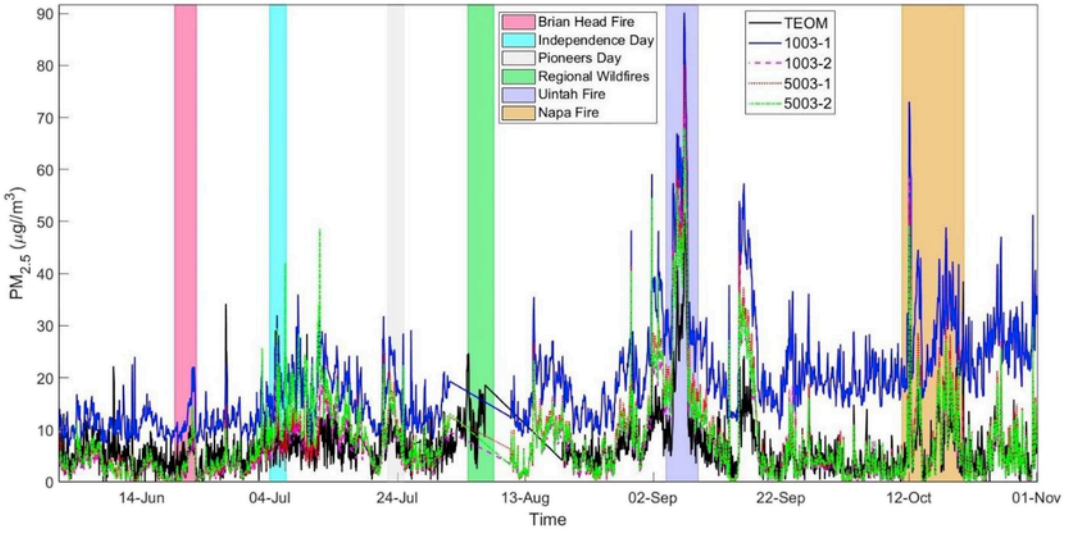

Fig. 3. Hourly $PM_{2.5}$ concentrations from the TEOM and co-located PMS sensors in wildfire season 2017.

PMS $PM_{2.5}$ measurements during winter (Tables S–1). The exponential model (fit 1) provides the best model to capture the non-linear shape of the experimental data over the entire concentration range during the CAP season. For TEOM concentrations less than 40 μg/m^3 (fit 2), a linear model captured the data trends best (Tables S–1).

Fig. S-12 shows the fits for the PMS $PM_{2.5}$ measurements in the winter of 2016 and 2017, and it shows two important trends. First, both the PMS 1003s overestimate $PM_{2.5}$ concentrations, as most data lie above the 45-degree line. Second, the sensor response did not change after one year. This was confirmed by a Student's t-test on the slope of linear fit 2 (p-values of 0.871 and 0.594 for 1003–1 and 1003–2, respectively). Fit 1 for the PMS 1003s suggests that 1003s overestimated the measurements of TEOM more in the winter of the first year than the second year, which may indicate a change in the performance of the sensor. However, the limited number of TEOM $PM_{2.5}$ concentrations above 40 μg/m^3 can have a large effect on the model fits, so additional data is needed to determine if the sensor performance is actually changing.

Fig. 4 compares the fitted lines for the two different sensor types in the winter of 2017. For concentrations up to 40 μg/m^3, the PMS 1003s overestimate $PM_{2.5}$ concentrations by a factor of 1.89. A Student's t-test showed no statistically significant difference in the slopes of the two PMS 1003s (p-value = 0.952). This overestimation was similar in 2016 (Kelly et al., 2017). The PMS 5003–1 overestimates $PM_{2.5}$ concentrations by a factor of 1.47, while the PMS 5003–2 roughly agrees with the FEM measurements (slope of 1.08). The slopes of PMS 5003s differ significantly (Student's t-test, p-value <0.001). A SQAMD study compared the PMS 1003 and 5003 to a FEM and also found that the PMS sensors generally overestimate $PM_{2.5}$ concentrations (SQAMD, 2016).

The PMS response to PM_{10} was linear in 2016 and 2017, during the winter season (Figs. S-13 and S-14). Fig. S-13 compares the linear relationship of the hourly FEM and PMS 1003 PM_{10} readings in 2016 and 2017. Comparing the slopes for the PMS 1003s in 2016 and 2017 showed no statistically significant difference (Student's t-test, p-values of 0.697 and 0.714 for 1003–1 and 1003–2, respectively). Fig. S-14 and Tables S–1 show that 1003s and 5003–1 overestimate the PM_{10} concentrations (fit 3 slopes of 1.45, 1.50, and 1.21 for 1003–1, 1003–2 and 5003–1, respectively) while 5003–2 roughly underestimated the PM_{10} TEOM data (fit 3 slope of 0.909).

Figs. S-15-17 show the diurnal variations of four meteorological factors (including RH, temperature, wind speed and wind direction) and the PM levels as well as the diurnal changes of the RMSE of the best fits for each sensor in each season. The PMS 1003–1 (sensor that drifted) RMSEs are higher in all seasons and exhibit different diurnal trends compared to the other PMS sensors. The RMSE of the fits show no consistent diurnal trends except for one strong peak in PM_{10} RMSE for all PMS sensors at noon. This was caused by the dust storm that occurred at noon on October 20, 2017 which increased the TEOM PM $_{2.5}$ and PM_{10} levels to 38.5 μg/m^3 and 472 μg/m^3, respectively. The diurnal changes of the meteorological factors in Figs. S-15-17 are typical for each season in this region. The diurnal wind pattern in this region is associated with cold air flowing down from the mountains into the valley in the morning and the evening. In winter 2017, $PM_{2.5}$ levels generally increase around 8 am and decrease around 7 pm which is likely associated with the traffic. The PM levels during spring and generally wildfire season do not seem to exhibit much diurnal pattern.

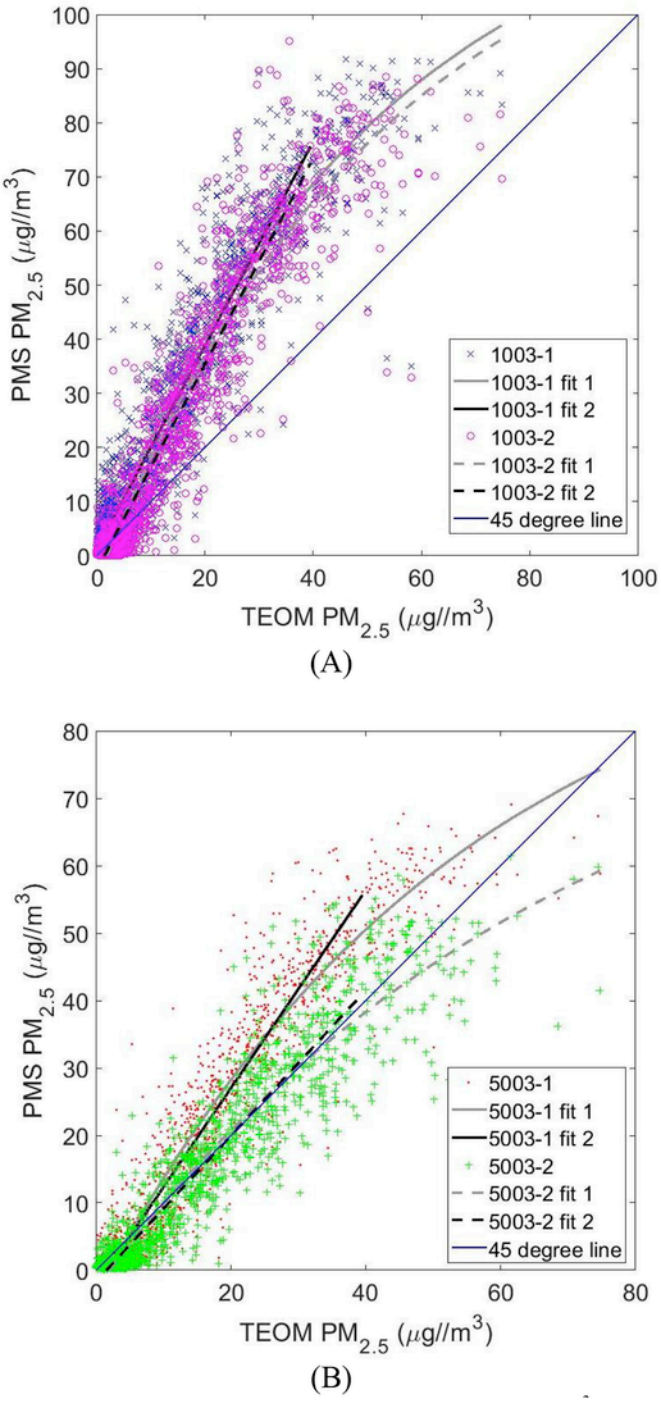

Fig. 4. Comparison of exponential (fit 1) and linear up to 40 μg/m^3 (fit 2) models fitted to FEM (TEOM) hourly $PM_{2.5}$ concentrations for PMS 1003s (A) and PMS 5003s (B) in winter 2017.

3.6. Bias

The hourly TEOM provided the reference concentrations for the bias determination (Eq. (2)). Table 3 summarizes bias estimates of the PMS sensors for 2016 and 2017, for the full dataset and for PMS measurements greater than the LOD (from Tables S–3) for each PMS sensor. The average mean bias for all PMS sensors in 2016 and 2017

Table 3
Bias estimates of hourly $PM_{2.5}$ concentration for the PMS sensors for all concentrations and for concentrations above each sensor's LOD.

year	Season	Data range	Parameters	1003–1	1003–2	5003–1	5003–2
2016	winter	All readings	Bias %	70.0	50.1	–	–
			Obs	736	684	–	–
			RMSE μg/m^3	17.0	14.8	–	–
			Norm RMSE %	73.8	62.8		
		Over LOD	Bias %	61.5	53.1	–	–
			Obs	395	364	–	–
			RMSE μg/m^3	21.9	19.3	–	–
			Norm RMSE %	59.4	51.0	–	–
2017	winter	All readings	Bias %	151	51.8	11.7	−14.2
			Obs	1588	1588	1588	1588
			RMSE μg/m^3	18.4	16.0	8.52	5.54
			Norm RMSE %	124	108	57.5	37.4
		Over LOD	Bias %	89.6	56.9	11.6	−18.4
			Obs	974	1107	1231	1299
			RMSE μg/m^3	23.0	19.1	9.60	6.09
			Norm RMSE %	103	94.1	51.7	34.3
	Spring	All readings	Bias %	252	−22.1	−22.9	−29.1
			Obs	1672	1700	1769	1769
			RMSE μg/m^3	18.4	16.0	8.52	5.54
			Norm RMSE %	124	108	57.5	37.4
		Over LOD	Bias %	−2.43	−37.8	−36.7	−42.6
			Obs	24	431	428	387
			RMSE μg/m^3	25.8	20.3	10.7	6.89
			Norm RMSE %	95.7	90.4	47.3	30.1
	Wildfire	All readings	Bias %	366	3.46	22.1	20.8
			Obs	3020	3009	3034	3035
			RMSE μg/m^3	15.1	5.05	5.80	5.40
			Norm RMSE %	225	74.8	86.1	80.2
		Over LOD	Bias %	122	−3.72	13.0	12.9
			Obs	417	2461	2454	2373
			RMSE μg/m^3	25.4	18.0	9.60	6.29
			Norm RMSE %	96.8	98.2	51.7	33.2

was 42.5%, which is less than the 475% reported for sixty-six Speck sensors from two outdoor campaigns (7 days with an average $PM_{2.5}$ concentration of 1.45 μg/m^3, Zikova et al., 2017). For PMS measurements greater than the LOD, the average mean bias for both years decreases to 20.2%. Zikova et al. (2017) also observed this strong connection between the hourly biases of the Speck measurements and the reference Grimm 1.109 monitor. In their outdoor campaign, the mean bias of the Speck sensors decreased to −29% by considering only 14 data points greater than the sensor LOD (10 μg/m^3). The mean biases of both 1003s increased in 2017 compared to 2016. However, it is unclear whether the sensor performance changed or the differences in the $PM_{2.5}$ concentrations during these two years led to this apparent change in performance.

PMS1003-1's response clearly drifted in spring and wildfire season; it had the highest mean bias among the four PMS sensors, 366%. This can also be seen in the intercept of the linear fit for PMS 1003–1, which increased to 10.6 μg/m^3 (Tables S–1). For values over the LOD, the mean bias of PMS 1003-1 dropped to 122%, but is still much greater than the other sensors (Fig. S-18).

3.7. Sensor stability and seasonal behavior

In order to evaluate the stability of the PMS sensors, the changes in their normalized residuals (Eq. (5)) were tracked over the course of the study. As shown in Fig. S-19, the magnitude of the normalized residuals slightly decreased for PMS 1003–2 and 5003s over the course of the study. This slight reduction in the magnitude of the normalized residual is statistically significant (Student's t-test, p-value = 0.001). During CAPs, the PMS sensors overestimate PM concentrations, and their response becomes nonlinear, thus decreasing the magnitude of residuals during the winter season. The lowest residuals for all sensors occurred during the Uintah wildfire, which substantially increased the PM concentrations in Salt Lake City. In addition, over time, as dust deposits on the sensor's photodetector, the PMS's response to light scattering may decline, thus lowering PM measurements and consequently the normalized residuals. After the sensors had been outside for several months (30 months for 1003s and 18 months for 5003s), three of the sensors were cleaned by blowing air inside the inlet and the fan, however, this limited evaluation of cleaning sensors with canned compressed air showed no improvement in the magnitude of residuals for the sensors after the cleaning (Fig. S-20). In fact, the residuals increased for a few days after cleaning. Blowing canned air into the sensor may have entrained PM deposited on the sensor surfaces, which may have remained in the laser chamber for some period of time. After two days, sensor 1003–2 and 5003–2 returned to their normal behavior but 5003-1 did not. It is possible that blowing air into that sensor could damage the fan. At this point, blowing air into the sensors is not recommended although this requires further investigation.

Fig. S-19 also shows the increase in the magnitude of the residuals for PMS 1003–1 as its response began to drift. As discussed with the wildfires, PMS 1003-1 measurements began drifting from PMS 1003–2 in March, and this drift continued through the end of October 2017 (Fig. 3). Subsequent inspection of the PMS 1003–1 identified a loose connection to the fan, causing the fan to behave erratically. It is possible that the erratic fan behavior caused some particles to be retained in the sensing chamber or that another problem such as a change in laser alignment led to an increased estimate of PM concentration.

We also considered how the PMS response varied seasonally by comparing the linear fits of the PMS sensors to the FEM results for each month of the study as well as the key contributions to $PM_{2.5}$

mass in 2017 (Tables S–2). This table shows that month-to-month responses compared to the FEM varied substantially. For example, the slopes in May are 2.23–4.70 times lower than the slopes in January. This is most likely due to the differences in both the concentration and composition of particles during the winter compared to the other seasons. Tables S–2 shows that secondary inorganic compounds (ammonium nitrate, ammonium sulfate, and ammonium chloride) are the main contributors to $PM_{2.5}$ during winter (greater than 61.1%), and during spring and wildfire season the secondary inorganic aerosols contribution decrease while contributions of elemental carbon, organic carbon and crustal material increase. This is particularly notable in September when the Uintah fire affected PM levels in Salt Lake City, and organic carbon contributed 63.4% of $PM_{2.5}$ mass.

4. Conclusion

Emerging technologies in low-cost, air-quality sensing offer the potential to provide improved spatiotemporal resolution PM measurements. This study focused on understanding the long-term performance of four low-cost light-scattering based sensors (Plantower PMS 1003s/5003s) under real world conditions during several CAPs, fireworks, wildfires and a dust storm. The Plantower PMS 1003 and 5003 provide good relative measures of $PM_{2.5}$. The results showed good correlations between the PMS sensors and the reference monitors ($PM_{2.5}$ FRM/FEM) in the winter season ($R^2 > 0.858$), substantial seasonal variation in sensor performance, high intra-sensor agreements ($R^2 > 0.970$), and drift in one sensor. The PMS sensors response to PM_{10} was poorer than to $PM_{2.5}$, and they failed to capture a 10-fold increase in PM_{10} associated with a dust storm, measured by the FEM. The different calibration factors for a same model of sensor indicates that a systematic laboratory calibration or an in situ calibration strategy is needed. The seasonal-dependence of the calibration factors illustrate the need for seasonal or condition-specific calibration. Finally, the identification of sensor drift suggests that regular evaluation of the sensor measurements, particularly at low PM levels, could be used to identify poorly functioning sensors. Overall, consideration of long-term sensor performance in the field is critical to understanding the measurements produced from networks of low-cost PM sensors.

Acknowledgement

We gratefully acknowledge NSF support under award numbers 1646408 and 1642513. Thanks to PurpleAir for providing sensors and to the Utah Division of Air Quality for allowing co-location of low-cost sensors at their monitoring station. Also, thanks to Shayne Ward with the Utah Division of Forestry, Fire & State Lands for providing the most recent information about the wildfires in the Utah State.

Appendix A. Supplementary data

Supplementary data to this article can be found online at https://doi.org/10.1016/j.envpol.2018.11.065.

References

Austin, E., Novosselov, I., Seto, E., Yost, M.G., 2015. Laboratory evaluation of the Shinyei PPD42NS low-cost particulate matter sensor. PLoS One 10, 1–17. https://doi.org/10.1371/journal.pone.0137789.

Baasandorj, M., Brown, S., Hoch, S., Crosman, E., Long, R., Silva, P., Mitchell, L., Hammond, I., Martin, R., Bares, R., Lin, J., Sohl, J., Page, J., McKeen, S., Pennell, C., Franchin, A., Petersen, R., Hallar, G., Fibiger, D., Womack, C., McDuffie, E., Moravek, A., Murphy, J., Hrdina, A., Thornton, J., Goldberger, L., Lee, B., Riedel, T., Whitehill, A., Kelly, K., Hansen, J., Eatough, D., 2018. 2017 Utah Winter Fine Particulate Study Final Report.

Barman, S.C., Singh, R., Negi, M.P.S., Bhargava, S.K., 2009. Fine particles (PM2.5) in ambient air of Lucknow city due to fireworks on Diwali festival. J. Environ. Biol. 30, 625–632.

Beard, J.D., Beck, C., Graham, R., Packham, S.C., Traphagan, M., Giles, R.T., Morgan, J.G., 2012. Winter temperature inversions and emergency department visits for asthma in Salt Lake County, Utah, 2003-2008. Environ. Health Perspect. 120, 1385–1390. https://doi.org/10.1289/ehp.1104349.

Brook, R.D., Rajagopalan, S., Iii, C.A.P., Brook, J.R., Bhatnagar, A., Diez-roux, A.V., Holguin, F., Hong, Y., Luepker, R.V., Mittleman, M.A., Peters, A., Siscovick, D., Smith, S.C., Whitsel, L., Kaufman, J.D., 2010. Particulate Matter Air Pollution and Cardiovascular Disease an Update to the Scientific Statement from the American. https://doi.org/10.1161/CIR.0b013e3181dbece1.

Dinoi, A., Donateo, A., Conte, M., Conte, M., Belosi, F., 2017. Comparison of atmospheric particle concentration measurements using different optical detectors: potentiality and limits for air quality applications. Meas. J. Int. Meas. Confed. 106, 274–282. https://doi.org/10.1016/j.measurement.2016.02.019.

Gao, M., Cao, J., Seto, E., 2015. A distributed network of low-cost continuous reading sensors to measure spatiotemporal variations of PM2.5 in Xi'an. China. Environ. Pollut. 199, 56–65. https://doi.org/10.1016/j.envpol.2015.01.013.

Hackmann, D., Sjöberg, E., 2017. Ambient air pollution and pregnancy outcomes—a study of functional form and policy implications. Air Qual. Atmos. Heal. 10, 129–137. https://doi.org/10.1007/s11869-016-0415-2.

Han, I., Symanski, E., Stock, T.H., 2017. Feasibility of using low-cost portable particle monitors for measurement of fine and coarse particulate matter in urban ambient air. J. Air Waste Manag. Assoc. 67, 330–340. https://doi.org/10.1080/10962247.2016.1241195.

Hänninen, O.O., Salonen, R.O., Koistinen, K., Lanki, T., Barregard, L., Jantunen, M., 2009. Population exposure to fine particles and estimated excess mortality in Finland from an East European wildfire episode. J. Expo. Sci. Environ. Epidemiol. 19, 414–422. https://doi.org/10.1038/jes.2008.31.

Health Effects Institute, 2010. Traffic-related Air Pollution: a Critical Review of the Literature on Emissions, Exposure, and Health Effects.

Holstius, D.M., Pillarisetti, A., Smith, K.R., Seto, E., 2014. Field calibrations of a low-cost aerosol sensor at a regulatory monitoring site in California. Atmos. Meas. Tech. 7, 1121–1131. https://doi.org/10.5194/amt-7-1121-2014.

Holstius, D.M., Reid, C.E., Jesdale, B.M., Morello-Frosch, R., 2012. Birth weight following pregnancy during the 2003 southern California wildfires. Environ. Health Perspect. 120, 1340–1345. https://doi.org/10.1289/ehp.1104515.

Jiao, W., Hagler, G., Williams, R., Sharpe, R., Brown, R., Garver, D., Judge, R., Caudill, M., Rickard, J., Davis, M., Weinstock, L., Zimmer-dauphinee, S., Buckley, K., 2016. Community Air Sensor Network (CAIRSENSE) Project : Evaluation of Low-cost Sensor Performance in a Suburban Environment in the Southeastern United States. 5281–5292. https://doi.org/10.5194/amt-9-5281-2016.

Jovašević-Stojanović, M., Bartonova, A., San Topalovi, C.C.,D., Lazovi, I., Pokri, B., Ristovski, Z., 2015. On the use of small and cheaper sensors and devices for indicative citizen-based monitoring of respirable particulate matter. Environ. Pollut. 206, 696–704. https://doi.org/10.1016/j.envpol.2015.08.035.

Kaiser, H., Specker, H., 1956. Bewertung und vergleich von analysenverfahren. Fresenius' Z. für Anal. Chem. 149, 46–66.

Kelly, K.E., Whitaker, J., Petty, A., Widmer, C., Dybwad, A., Sleeth, D., Martin, R., Butterfield, A., 2017. Ambient and laboratory evaluation of a low-cost particulate matter sensor. Environ. Pollut. 221, 491–500. https://doi.org/10.1016/j.envpol.2016.12.039.

Kolbe, A., Gilchrist, K.L., 2009. An extreme bushfire smoke pollution event: health impacts and public health challenges. NSW Public Health Bull. 20, 19. https://doi.org/10.1071/NB08061.

Kunii, O., Kanagawa, S., Yajima, I., Hisamatsu, Y., Yamamura, S., Amagai, T., Ismail, I.T.S., 2002. The 1997 haze disaster in Indonesia: its air quality and health effects. Arch. Environ. Health 57, 16–22. https://doi.org/10.1080/00039890209602912.

Li, J., Biswas, P., 2017. Optical characterization studies of a low-cost particle sensor. Aerosol Air Qual. Res. 17, 1691–1704. https://doi.org/10.4209/aaqr.2017.02.0085.

Liu, D., Zhang, Q., Jiang, J., Chen, D.R., 2017. Performance calibration of low-cost and portable particular matter (PM) sensors. J. Aerosol Sci. 112, 1–10. https://doi.org/10.1016/j.jaerosci.2017.05.011.

Lucie, D., 2017. Haboob sweeps over Salt Lake city, [WWW Document]. Salt Lake City Haboob. URL https://www.abc4.com/weather/haboob-sweeps-over-salt-lake-city/841368664, (accessed 11.13.2018).

Manikonda, A., Zikova, N., Hopke, P.K., Ferro, A.R., 2016. Laboratory assessment of low-cost PM monitors. J. Aerosol Sci. 102, 29–40. https://doi.org/10.1016/j.jaerosci.2016.08.010.

Mukherjee, A., Stanton, L., Graham, A., Roberts, P., 2017. Assessing the utility of low-cost particulate matter sensors over a 12-week period in the Cuyama Valley of California. Sensors 17, 1805. https://doi.org/10.3390/s17081805.

Papapostolou, V., Zhang, H., Feenstra, B.J., Polidori, A., 2017. Development of an environmental chamber for evaluating the performance of low-cost air quality sen-

sors under controlled conditions. Atmos. Environ. 171, 82–90. https://doi.org/10.1016/j.atmosenv.2017.10.003.
Patel, S., Li, J., Pandey, A., Pervez, S., Chakrabarty, R.K., Biswas, P., 2017. Spatio-temporal measurement of indoor particulate matter concentrations using a wireless network of low-cost sensors in households using solid fuels. Environ. Res. 152, 59–65. https://doi.org/10.1016/j.envres.2016.10.001.
Piedrahita, R., Xiang, Y., Masson, N., Ortega, J., Collier, A., Jiang, Y., Li, K., Dick, R.P., Lv, Q., Hannigan, M., Shang, L., 2014. The next generation of low-cost personal air quality sensors for quantitative exposure monitoring. Atmos. Meas. Tech 7, 3325–3336. https://doi.org/10.5194/amt-7-3325-2014.
Pope, C.A., Muhlestein, J.B., May, H.T., Renlund, D.G., Anderson, J.L., Horne, B.D., 2006. Ischemic heart disease events triggered by short-term exposure to fine particulate air pollution. Circulation 114, 2443–2448. https://doi.org/10.1161/CIRCULATIONAHA.106.636977.
PurpleAir, 2018. PurpleAir Map, air quality Map, [WWW Document]. URL http://map.purpleair.org/, (accessed 1.3.2018).
Raaschou-Nielsen, O., Andersen, Z.J., Beelen, R., Samoli, E., Stafoggia, M., Weinmayr, G., Hoffmann, B., Fischer, P., Nieuwenhuijsen, M.J., Brunekreef, B., Xun, W.W., Katsouyanni, K., Dimakopoulou, K., Sommar, J., Forsberg, B., Modig, L., Oudin, A., Oftedal, B., Schwarze, P.E., Nafstad, P., De Faire, U., Pedersen, N.L., Östenson, C.-G., Fratiglioni, L., Penell, J., Korek, M., Pershagen, G., Eriksen, K.T., Sørensen, M., Tjønneland, A., Ellermann, T., Eeftens, M., Peeters, P.H., Meliefste, K., Wang, M., Bueno-de-Mesquita, B., Key, T.J., de Hoogh, K., Concin, H., Nagel, G., Vilier, A., Grioni, S., Krogh, V., Tsai, M.-Y., Ricceri, F., Sacerdote, C., Galassi, C., Migliore, E., Ranzi, A., Cesaroni, G., Badaloni, C., Forastiere, F., Tamayo, I., Amiano, P., Dorronsoro, M., Trichopoulou, A., Bamia, C., Vineis, P., Hoek, G., 2013. Air pollution and lung cancer incidence in 17 European cohorts: prospective analyses from the European study of cohorts for air pollution effects (ESCAPE). Lancet Oncol. 14, 813–822. https://doi.org/10.1016/S1470-2045(13)70279-1.
Shapiro, M.A., Swann, P.G., Hartsough, M., 2014. Regulatory considerations of lower cost air pollution sensor data performance. Handb. Ther. Antibodies 1, 277–300. https://doi.org/10.1002/9783527619740.ch12.
Sousan, S., Koehler, K., Hallett, L., Peters, T.M., 2017. Evaluation of consumer monitors to measure particulate matter. J. Aerosol Sci. 107, 123–133. https://doi.org/10.1016/j.jaerosci.2017.02.013.
Sousan, S., Koehler, K., Thomas, G., Park, J.H., Hillman, M., Halterman, A., Peters, T.M., 2016. Inter-comparison of low-cost sensors for measuring the mass concentration of occupational aerosols. Aerosol Sci. Technol. 50, 462–473. https://doi.org/10.1080/02786826.2016.1162901.
SQAMD, 2016. Field Evaluation of SENS-IT Sensor Background.
Steenburgh, J., 2017. Wasatch Weather Weenies, [WWW Document]. Wasatch Weather Weenies http://wasatchweatherweenies.blogspot.com/2017/10/postfrontal-dustpocalypse.html, (accessed 9.11.2018).
Steinle, S., Reis, S., Eric, C., 2013. Science of the total environment quantifying human exposure to air pollution — moving from static monitoring to spatio-temporally resolved personal exposure assessment. Sci. Total Environ. 443, 184–193. https://doi.org/10.1016/j.scitotenv.2012.10.098.
Utah Division of Air Quality, 2017. Utah Division of Air Quality Western Wildfire Smoke Exceptional Events. Salt Lake City.
Vahlsing, C., Smith, K.R., 2012. Global review of national ambient air quality standards for PM10 and SO2 (24 h). Air Qual. Atmos. Heal. 5, 393–399. https://doi.org/10.1007/s11869-010-0131-2.
Wang, Y., Li, J., Jing, H., Zhang, Q., Jiang, J., Biswas, P., 2015. Laboratory evaluation and calibration of three low-cost particle sensors for particulate matter measurement. Aerosol Sci. Technol. 49, 1063–1077. https://doi.org/10.1080/02786826.2015.1100710.
Weuve, J., Puett, R.C., Schwartz, J., Yanosky, J.D., Laden, F., Grodstein, F., 2012. Exposure to particulate air pollution and cognitive decline in older women. Arch. Intern. Med. 172, 219. https://doi.org/10.1001/archinternmed.2011.683.
Williams, R., Kaufman, A., Hanley, T., Rice, J., Garvey, S., 2014. Evaluation of Field-deployed Low Cost PM Sensors, doi:EPA/600/R-14/464 (NTIS PB 2015-102104).
Zheng, T., Bergin, M.H., Johnson, K.K., Tripathi, S.N., Shirodkar, S., Landis, M.S., Sutaria, R., Carlson, D.E., 2018. Field Evaluation of Low-cost Particulate Matter Sensors in High- and Low-concentration Environments. 4823–4846.
Zhu, K., Zhang, J.J., Lioy, P.J., Zhu, K., Zhang, J.J., Lioy, P.J., 2012. Evaluation and Comparison of Continuous Fine Particulate Matter Monitors for Measurement of Ambient Aerosols Evaluation and Comparison of Continuous Fine Particulate Matter Monitors for Measurement of Ambient Aerosols 2247. https://doi.org/10.3155/1047-3289.57.12.1499.
Zikova, N., Hopke, P.K., Ferro, A.R., 2017. Evaluation of new low-cost particle monitors for PM2.5 concentrations measurements. J. Aerosol Sci. 105, 24–34. https://doi.org/10.1016/j.jaerosci.2016.11.010.

E T O C B L U R B

This study identified strong correlations between the Plantower sensors and reference monitors during two winters, substantial differences in seasonal responses, and significant intra-sensor variability.